Chemical Physics Letters 528 (2012) 39–43

Contents lists available at SciVerse ScienceDirect

Chemical Physics Letters

journal homepage: www.elsevier.com/locate/cplett

Shell magnetism in transition metal doped calcium superatom

Vikas Chauhan [a], Victor M. Medel [b], J. Ulises Reveles [b,*], Shiv N. Khanna [b,*], Prasenjit Sen [a]

[a] Harish-Chandra Research Institute, Chhatnag Road Jhunsi, Allahabad 211019, India
[b] Department of Physics, Virginia Commonwealth University, Richmond, VA 23284, USA

ARTICLE INFO

Article history:
Received 17 October 2011
In final form 12 January 2012
Available online 21 January 2012

ABSTRACT

Clusters of metallic elements with valence electron counts 2, 8, 18, 20, ... are known to be stable with filled electronic shells and large gaps between shells. Through first principles theoretical studies of $TMCa_8$ (TM = Sc, Ti, V, Cr, Mn, Fe, Co, ...) clusters we identify a stable magnetic $FeCa_8$ cluster of 24 valence electrons distributed into a closed $1S^2\ 1P^6\ 1D^{10}\ 2S^2$ shell sequence and with four electrons occupying the majority $2D_{xy}$, $2D_{x^2-y^2}$, $2D_{xz}$ and $2D_{yz}$ levels while the unfilled $2D_{z^2}$ level is separated by a large energy gap of 0.61 eV arising from atomic deformation and exchange splitting.

1. Introduction

An important direction in the field of clusters is to synthesize materials where atomic clusters serve as the primary building blocks. Since the properties of clusters can change with size, composition, and the charged state, homogeneous or heterogeneous clusters can allow atomistic control over the properties of the resulting material [1–4]. Identifying stable species that will retain their characteristics on assembly is the first step towards such an objective [5–9]. It was early on that experiments on the mass spectra, ionization potentials, and chemical reactivity, all pointed that small clusters of metallic elements exhibited stability at electron counts 2, 8, 18, 20, 34, 40, 58, ... Concurrently, Knight and coworkers proposed a simple Jellium model to account for the observations [10,11]. In this model, the positive charge of the ionic cores is spread uniformly over a sphere of radius determined by the cluster size. The electronic states for such a potential bunch into 1S, 1P, 1D, 2S, 1F, 2P, ... shells whose filling coincided with the observed electron counts and hence could account for the observed magic species [12–16]. More interestingly, later studies indicated that clusters with open shells had electronic features similar to the case of atoms with similar valence character. For example, an Al_{13} with 39 valence electrons distributed in $1S^2\ 1P^6\ 1D^{10}\ 2S^2\ 1F^{14}\ 2P^5$ superatomic shell had an electron affinity close to a halogen (Cl) atom [17,18]. The grouping of electronic states into shells and similarities in behavior of open shells of a given angular momentum in clusters and atoms, prompted Khanna and Jena to propose that stable clusters could be regarded as superatoms forming a 3rd dimension to the periodic table [17]. First principles electronic structure calculations on numerous symmetric metal clusters show that, despite being highly simplistic and marked by indisputable limitations, the Jellium model continues to provide a reasonable account of the grouping of electronic states into shells and the shape of the electronic orbitals in a variety of clusters.

Since the clusters with filled shells are stable, there has been a constant search to explore if stable clusters at electron counts different from the above could be found. It was quite early on that it was realized that deformation of the Jellium potential can lead to splitting of Jellium levels and consequently stabilize subshell closings [19,20]. For example, a deformation of the spherical potential into oblate geometries can split the P_z and D_z^2 states. A recent example is $Al_{22}Cu^-$ that is found to demonstrate unusual stability in experiments reacting clusters with oxygen [21]. The cluster has 68 valence electrons, and as we recently showed, the introduction of Cu induces an oblate deformation resulting in splitting of the D_{z^2} level that can also be looked upon as a crystal field splitting and accounts for its uncommon stability. A similar model also accounts for the stability of a planar Au_6Mn molecule where the in-plane P and D orbitals are stabilized as compared to the P_z and D_{xz}, D_{yz}, and D_{z^2} orbitals, respectively [20].

The electronic orbitals in superatoms, while resembling those in real atoms in shape, do spread over multiple atoms. The filling of electronic shells generally do not follow the Hund's rule of maximizing the spin. This is because, as discussed above, the geometrical distortions can remove the degeneracies in electronic shells and stabilize the clusters via Jahn–Teller effect [22]. This leads to electronic-orbitals that are filled with pairs of electrons and are nonmagnetic. Stable magnetic clusters composed of semiconducting elements, such as $MnGe_{12}$ or $MnSn_{12}$ have previously been reported and were termed as Magnetic Superatoms [7]. The term 'superatom' as originally introduced by Khanna and Jena [5], however, refers to clusters with valence pool forming a nearly free electron gas where the quantum confinement results in bunching of electron states into shells. Within such a framework, we recently

* Corresponding authors.
E-mail addresses: jureveles@vcu.edu (J. Ulises Reveles), snkhanna@vcu.edu (S.N. Khanna).

0009-2614/$ - see front matter © 2012 Elsevier B.V. All rights reserved.
doi:10.1016/j.cplett.2012.01.034

proposed that magnetic superatoms with spin moments could be stabilized by inducing spin dependent splitting of supershells [23]. This can be accomplished by hybridizing the superatomic orbitals with atomic orbitals of atoms with large exchange splitting [23,24]. We demonstrated this intriguing phenomenon in $FeMg_8$ clusters where the exchange split atomic d-states of transition metal (TM) hybridize with D-orbitals of the superatom leading to superatom orbitals of D character that have large exchange splitting, and fill to maximize the total spin as in Hund's rule in atoms. The cluster has a highly symmetric structure consisting of a square antiprism of Mg atoms containing an interior Fe atom. Are there other such highly symmetric endohedral clusters that exhibit magnetic character?

The purpose of this Letter is to offer an interesting example where the crystal field splitting compounded with exchange coupling, lead to a magnetic superatom extending our earlier investigations to other group two elements [24]. We demonstrate our intriguing finding by examining the stability of transition metal doped calcium $TMCa_n$ clusters containing various 3d transition metal atoms and 6–10 Ca atoms. We identify $FeCa_8$ with 24 valence electrons as a highly stable cluster that has a closed shell of 20 paired electrons and four un-paired electrons occupying the $2D_{xy}$, $2D_{x^2-y^2}$, $2D_{xz}$ and $2D_{yz}$ levels, while the $2D_{z^2}$ level is separated by a large energy gap. We show that the crystal field splitting and the exchange splitting act together to stabilize this magnetic species. Section 2 describes our theoretical methodology, Section 3 discusses our results and conclusions are presented in Section 4.

2. Theoretical methodology

First principles electronic structure calculations on $TMCa_8$ (TM = Sc, Ti, V, Cr, Mn, Fe, Co, Ni, Cu and Zn) and $FeCa_n$ (n = 6–10) clusters were performed within the generalized gradient density functional theory (DFT) formalism. The calculations were carried out using the linear combination of Gaussian type orbitals centered at the atomic positions, employing the DFT Kohn–Sham code deMon2k [25]. The exchange and correlation effects were incorporated through the functional proposed by Perdew et al. [26]. A variational fitting of the Coulomb potential was employed in order to avoid the calculation of four-center electron repulsion integrals [27]. The exchange–correlation potential was calculated via a numerical integration from the orbital density. All electrons were treated explicitly using the double-ζ valence plus polarization (DZVP) basis sets [28]. The auxiliary density was expanded in primitive Hermite Gaussian functions using the GEN-A2 auxiliary function set that contains s, p, d, f and g auxiliary functions, and adapts automatically to the chosen orbital basis set [29]. To determine the ground state geometries and lowest energy excited states, several initial configurations were tried and fully optimized fixing their possible spin states and employing a quasi-Newton method in delocalized internal coordinates [30] without symmetry constraints. Resulting stationary points were ascertained via a frequency analysis.

3. Results and discussion

In all $TMCa_8$ (TM = Sc, Ti, V, Cr, Mn, Fe, Co, Cu and Zn) clusters, the ground state was found to be a square antiprism like arrangement of eight Ca atoms with an endohedral TM atom, similar to those previously reported for $TMMg_8$ species [24], with the exception of $NiCa_8$ which presented a capped octahedral geometry with singlet multiplicity. We would like to add that our studies also predict a nearly degenerate isomer (0.03 eV less stable) with a square antiprism structure and a spin magnetic moment of 2 μ_B for $NiCa_8$. All clusters optimized to a D_{4d} symmetry structure, with the exception of $CrCa_8$ and $CoCa_8$ that optimized to lower D_4 symmetry, $NiCa_8$ that optimized to a C_{2v} symmetry and $CuCa_8$ that optimized to a D_{2d} symmetry, as shown in Supplementary Fig. S1. The average Ca–Ca bond length ranges from 3.78 to 4.16 Å, and the average TM–Ca bond ranges from 2.94 to 3.42 Å. As our primary goal was to identify stable magnetic clusters, we proceeded to examine (1) the gap between the highest occupied and lowest unoccupied molecular orbitals (HOMO–LUMO gap), (2) the magnetic moment of the clusters, (3) the spin excitation energy representing the energy required to excite the cluster from the ground state to the next closest multiplicity and (4) the binding energy of the transition metal atom to the cluster. A large HOMO–LUMO gap is commonly a signature of chemical stability as a large gap indicates resilience to gain or lose charge as well as deformations of the electron cloud. Figure 1a presents the variation of HOMO–LUMO gap as a function of the TM atom in the $TMCa_8$ series. Note that $TiCa_8$, $FeCa_8$ and $ZnCa_8$ show larger gap compared to their neighbors. Figure 1b shows the spin magnetic moment of the clusters. Both the $TiCa_8$ and $ZnCa_8$ have singlet ground states while $FeCa_8$ has a spin magnetic moment of 4 μ_B. We also examined the spin excitation energy, ΔE_{spin}, representing the energy difference between the ground state and the nearest different spin configuration. Figure 1c shows the spin excitation energy. A large ΔE_{spin} indicates the robustness of the ground state multiplicity towards spin excitation. Finally Figure 1d represents the binding energy of the TM atom to the Ca_8 cluster calculated using the equation:

$$BE = E(Ca_8) + E(TM) - E(TMCa_8) \quad (1)$$

where $E(Ca_8)$, $E(TM)$ and $E(TMCa_8)$ are the total energies of the Ca_8 cluster, TM atom and the $TMCa_8$ cluster, respectively. Note that the passage from Mn to Fe leads to an increase in BE. Whereas it stays almost constant in going to Co. Based on all the above information, $FeCa_8$ is a unique cluster that has high HOMO–LUMO gap, spin excitation energy, a large spin magnetic moment and a high BE, and hence emerges as a likely candidate for a magnetic superatom.

To examine the microscopic mechanism underlying its stability, we analyzed the one electron levels and the associated electronic orbitals. We identified the angular momentum character of the orbitals by inspection of their global shape and nodes in analogy with atomic orbitals. Figure 2 shows the one electron levels and the molecular orbitals for $FeCa_8$. The lowest state has 1S character and is spread out over the whole cluster. The next majority states are 1D states while the minority group has two degenerate states that have a $1P_x$ and $1P_y$ character. The oblate shape of the cluster broke the degeneracy of the 1P orbitals and pushed the $1P_z$ around 0.45 eV higher in energy. The same occurs in majority 1D orbitals in which again the degeneracy has been broken into two groups of 4 and 1 orbitals, characteristic of a crystal field splitting for an oblate geometry. The filling of majority and minority orbitals leads to $1S^2$ $1P^6$ $1D^{10}$ $2S^2$ orbitals filled with paired electrons. Since the system has 24 valence electrons, one is left with four electrons past the filled shell. Note that the majority 2D-states are split into a group of 4 ($2D_{xy}$, $2D_{x^2-y^2}$, $2D_{xz}$ and $2D_{yz}$) and a $2D_{z^2}$ state. Furthermore, the large exchange splitting between the spin up and spin down electrons in a Fe atom induces a large exchange splitting in 2D states that are formed from hybridization between the atomic orbitals centered on Fe and those on Ca sites. Hence, the extra four electrons occupy the majority group of four 2D orbitals, and the $2D_{z^2}$ is placed around 0.6 eV higher in energy being the LUMO. The resulting species is a stable magnetic cluster with a spin magnetic moment of 4.0 μ_B for which the stability is rooted on the sub-orbital splittings arising from the geometrical distortion, as well as exchange splitting through hybridization between Fe 3d and the superatomic orbitals. A close atomic analog of $FeMg_8$ is an iron

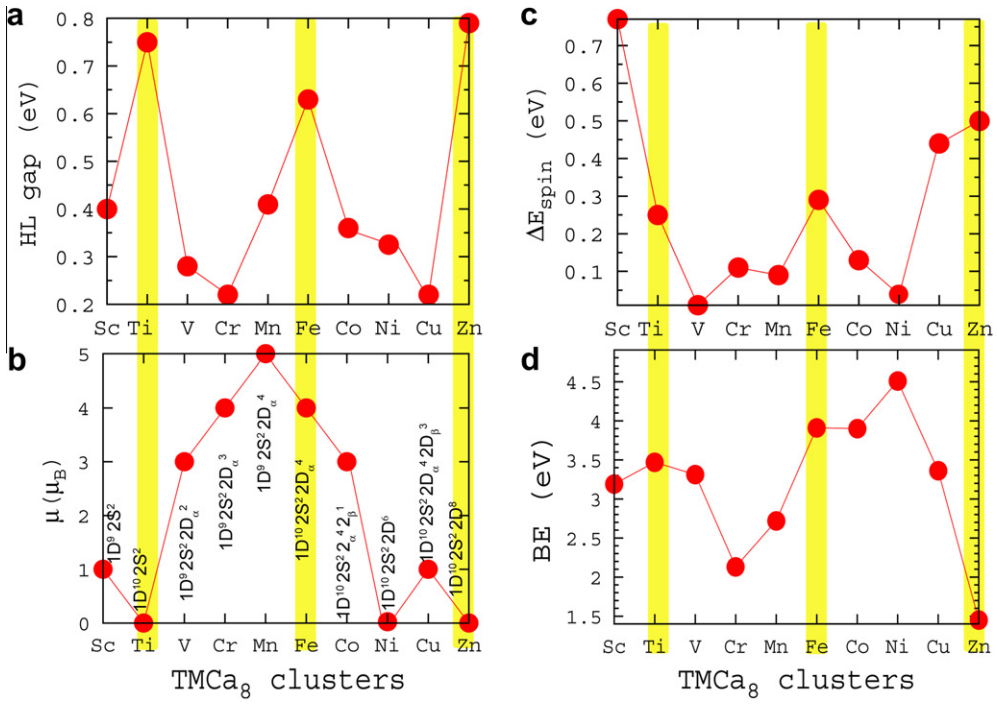

Figure 1. Energetic and magnetic trends of $TMCa_8$ clusters. (a) Variation of the HOMO–LUMO gap (HL gap) with the TM atom. (b) Variation of the magnetic moments (μ) with the TM atom and nature of frontier orbitals. (c) Variation of the relative energy between the ground state and the nearest isomer ΔE_{spin} as a function of the TM atom. (d) Variation of the binding energy BE with the TM atom.

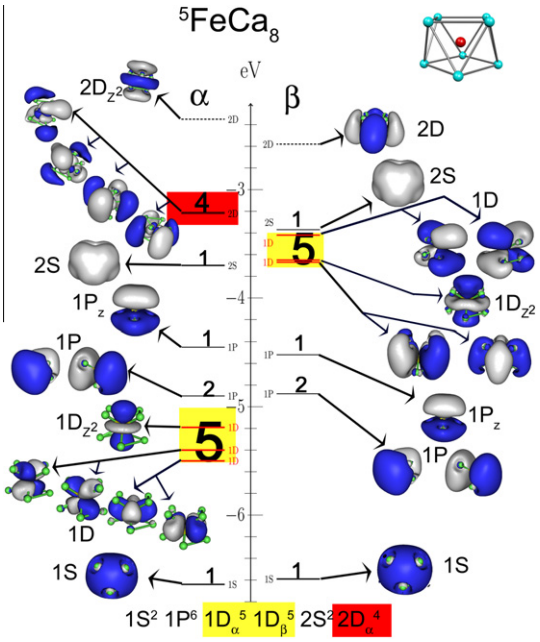

Figure 2. One electron energy levels and orbital wavefunction isosurfaces (isoval = 0.01 a.u.) in the $FeCa_8$ cluster. The majority and minority levels are shown. Continuous lines correspond to the filled levels while the dotted lines correspond to the unfilled states. For each level, the angular momentum of the supershells has been marked. The 1D occupied energy levels are highlighted in yellow and the red square shows the energy levels that contribute to the magnetic moment. The ground state geometry of the $FeMg_8$ cluster is also shown. (For interpretation of the references to color in this figure legend, the reader is referred to the web version of this article.)

atom, that has an electronic configuration $4s^2 3d^6$ with four unpaired d electrons and a spin magnetic moment of 4.0 μ_B.

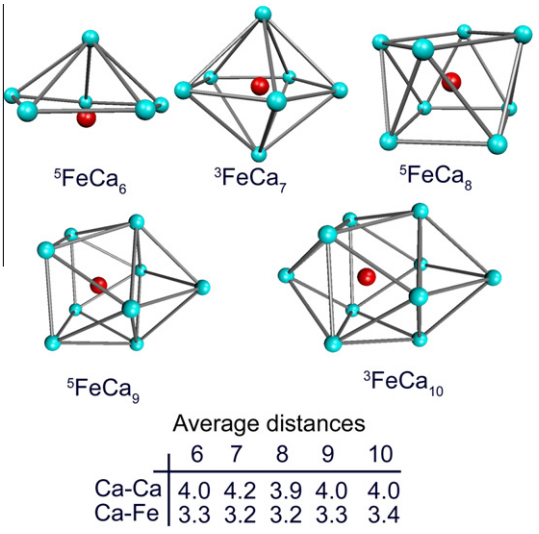

Figure 3. Ground state energy structures of $FeCa_n$ (n = 6–9) clusters. The average Ca–Ca and Ca–Fe bond lengths in Å are also given.

In the above, we examined the stability by comparing the progressions across the 3d series. We also wanted to examine whether $FeCa_8$ would be stable if we changed the number of Ca atoms. To this end, we examined the structure and stability of $FeCa_n$ (n = 6, 7, 8, 9 and 10) series. Figure 3 presents the calculated ground state geometries. $FeCa_6$ is a pentagonal pyramid with a Fe occupying the center of the base. $FeCa_7$ is the first clusters with an interior Fe atom with pentagonal bipyramid geometry. $FeCa_8$ is a square antiprism with an endohedral Fe atom, and both $FeCa_9$ and $FeCa_{10}$ are formed by capping opposite sites of $FeCa_8$. The average Ca–Ca bond length is around 4 Å, and the Ca–Fe bond 3.3 Å. To examine the chemical and magnetic stability, we monitored the variations

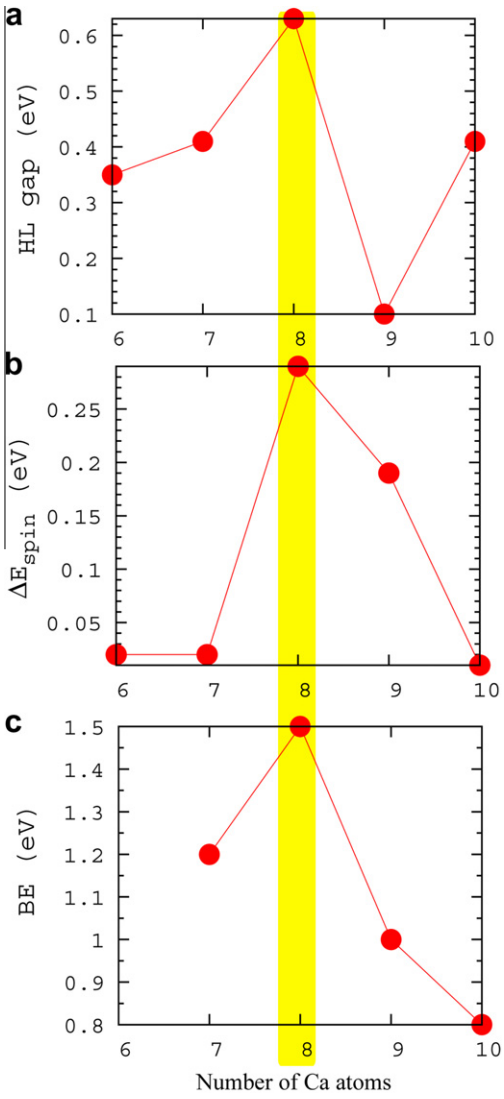

Figure 4. Energetic and magnetic trends of $FeCa_n$ (n = 6–9) clusters. (a) Variation of the HOMO–LUMO gap (HL gap) vs. the number of Ca atoms. (b) Variation of the relative energy between the ground state and the nearest isomer ΔE_{spin} as a function of the number of Ca atoms. (c) Variation of the energy gain ΔE upon successive addition of Ca atoms with n.

of HOMO–LUMO gap and ΔE_{spin} as a function of the number of Ca atoms in the $FeCa_n$ series. Figure 4a and b show distinct maxima for $FeCa_8$ suggesting its chemical stability with a robust spin state. To further prove the energetic stability of $FeCa_8$, we calculated the change in incremental binding energy ΔE_n as successive Ca atoms are added to a $FeCa_n$ species using the equation:

$$\Delta E_n = E(Ca) + E(FeCa_{n-1}) - E(FeCa_n). \quad (2)$$

Here E(Ca), $E(FeCa_{n-1})$, $E(FeCa_n)$ are the total energies of a Ca atom, $FeCa_{n-1}$ cluster, and $FeCa_n$ cluster, respectively. Figure 4c shows a maximum for $FeCa_8$ with large energy gain by adding a Ca atom to $FeCa_7$, and a low energy gain in adding an additional Ca atom. The maxima and a sharp drop in the incremental binding energy are both characteristics associated to enhanced stability of clusters [16,23,24].

To summarize, the present work demonstrate how the geometrical distortions can lift the degeneracy of electronic shells in clusters and how the sub-shells can be further split through hybridization with atomic orbitals of atoms with large exchange splitting. The result is a new set of stable clusters with differing origins of stability. In this work, we have demonstrated these interesting effects through $TMCa_8$ clusters. As shown by the analysis of the one electron levels and the associated electronic orbitals $TiCa_8$ with 20 valence electrons has a closed electronic shell $1S^2$ $1P^6$ $1D^{10}$ $2S^2$ electronic configuration. Replacing Ti by Fe adds four valence electrons and ordinarily should not be a stable species. However, the Fe atom enhances exchange splitting in supershells leading to a stable $FeCa_8$ magnetic superatom where the filling of majority super orbitals result in a magnetic species with a spin magnetic moment of 4.0 μ_B, and that mimics the properties of an Fe atom. Calculations of the $(FeCa_8)_2$ dimer, starting from two motifs, indicate that the individual clusters do retain their shape and have a ferromagnetic (FM) configuration with a spin magnetic moment of 8.0 μ_B as the lowest state. An antiferromagnetic (AF) state is only 0.021 eV higher in energy as shown in Supplementary Fig. S2. We are in the process of investigating the spin transport in dimers, and the magnetic ordering and the spin transport in bigger combinations of these magnetic motifs, and hope that the present investigations would stimulate experimental studies to verify these intriguing behaviors.

Acknowledgment

We gratefully acknowledge support from US Department of Energy (DOE) through Grant DE-FG02-11ER16213.

Appendix A. Supplementary data

Supplementary data associated with this article can be found, in the online version, at doi:10.1016/j.cplett.2012.01.034.

References

[1] S.J. Riley, E.K. Parks, G.C. Nieman, L.G. Pobo, S. Wexler, J. Chem. Phys. 80 (1984) 1360.
[2] M.E. Geusic, M.D. Morse, R.E. Smalley, J. Chem. Phys. 82 (1985) 590.
[3] D.J. Trevor, R.L. Whetten, D.M. Cox, A. Kaldor, J. Am. Chem. Soc. 107 (1985) 518.
[4] P. Jena, S.N. Khanna, B.K. Rao, Physics and Chemistry of Finite Systems: from Clusters to Crystals, World Scientific, Singapore, 1992.
[5] S.N. Khanna, P. Jena, Phys. Rev. Lett. 69 (1992) 1664.
[6] A. Perez et al., J. Phys. D: Appl. Phys. 30 (1997) 709.
[7] V. Kumar, Y. Kawazoe, Appl. Phys. Lett. 83 (2003) 2677.
[8] S.A. Claridge, A.W. Castleman Jr., S.N. Khanna, C.B. Murray, A. Sen, P.S. Weiss, ACS Nano 3 (2009) 244.
[9] N.K. Chaki et al., ACS Nano 4 (2010) 5813.
[10] W.D. Knight, K. Clemenger, W.A. De Heer, W.A. Saunders, M.Y. Chou, M.L. Cohen, Phys. Rev. Lett. 52 (1984) 2141.
[11] W.D. Knight, W.A. De Heer, W.A. Saunders, K. Clemenger, M.Y. Chou, M.L. Cohen, Chem. Phys. Lett. 134 (1987) 1.
[12] E. Janssens, S. Neukermans, S.P. Lievens, Curr. Opin. Solid State Mater. Sci. 8 (2004) 185.
[13] M.L. Kimble, A.W. Castleman Jr., J.U. Reveles, S.N. Khanna, Collect. Czech. Chem. Commun. 72 (2007) 185.
[14] J. Hartig, A. Stösser, P. Hauser, H. Schnöckel, Angew. Chem., Int. Ed. 46 (2007) 1658.
[15] M. Walter et al., Proc. Natl. Acad. Sci. USA 105 (2008) 9157.
[16] C.E. Jones Jr., P.A. Clayborne, J.U. Reveles, J.J. Melko, U. Gupta, S.N. Khanna, A.W. Castleman Jr., J. Phys. Chem. A 112 (2008) 13316.
[17] S.N. Khanna, P. Jena, Phys. Rev. B 51 (1995) 13705.
[18] D.E. Bergeron, A.W. Castleman, T. Morisato, S.N. Khanna, Science 304 (2004) 84.
[19] M. Kosinen, P. Lipas, M. Manninen, Z. Phys, D Atom. Mol. Cl. 35 (1995) 285.
[20] T. Höltz, P. Lievens, T. Vezprémi, M.T. Nguyen, J. Phys. Chem. C 113 (2009) 21016.
[21] P.J. Roach, W.H. Woodward, A.C. Reber, S.N. Khanna, A.W. Castleman Jr., Phys. Rev. B 81 (2010) 195404.
[22] S.N. Khanna, B.K. Rao, P. Jena, J.L. Martins, Jahn-Teller distortion, Hund's coupling and metastability in alkali tetramers, in: P. Jena, B.K. Rao, S.N. Khanna (Eds.), Physics and Chemistry of Small Clusters, Plenum Press, New York, 1987, pp. 435–438.
[23] J.U. Reveles, P.A. Clayborne, A.C. Reber, K. Pradhan, P. Sen, S.N. Khanna, Nat. Chem. 1 (2009) 310.
[24] V.M. Medel, J.U. Reveles, S.N. Khanna, V. Chauhan, P. Sen, A.W. Castleman Jr., Proc. Natl. Acad. Sci. USA 108 (2011) 10062.

[25] A.M. Köster, P. Calaminici, M.E. Casida, R. Flores-Moreno, G. Geudtner, A. Goursot, T. Heine, A. Ipatov, F. Janetzko, J.M. del Campo, S. Patchkovskii, J.U. Reveles, D.R. Salahub, A. Vela, deMon2k, V. 2.3.6, The deMon Developers Community: Cinvestav, México, 2006; available at <www.deMon-software.com>.
[26] J.P. Perdew, K. Burke, M. Ernzerhof, Phys. Rev. Lett. 77 (1996) 3865.
[27] B.I. Dunlap, J.W.D. Connolly, J.R. Sabin, J. Chem. Phys. 71 (1979) 3396.
[28] N. Godbout, D.R. Salahub, J. Andzelm, E. Wimmer, Can. J. Chem. 70–2 (1992) 560.
[29] P. Calaminici, F. Janetzko, A.M. Köster, R. Mejia-Olvera, B. Zúñiga-Gutierrez, J. Chem. Phys. 126 (2007) 044108.
[30] J.U. Reveles, A.M. Köster, J. Comp. Chem. 25 (2004) 1109.